

Geogas prospecting for buried deposits under loess overburden: Taking Shenjiayao gold deposit as an example

Mei Lu^{a,b}, Rong Ye^{a,*}, Zhenkai Wang^a, Xiaojia Wang^a

^a School of Earth Sciences and Resources, China University of Geosciences, Beijing 100083, China

^b Department of Geosciences, Auburn University, AL 36849, United States



ARTICLE INFO

Keywords:

Geogas prospecting
Nanoparticle
Deep-penetrating geochemical exploration
Geochemical anomaly
Gold ore deposit

ABSTRACT

The loess areas cover about 6% of China's land and they are thought to have a high likelihood of hosting valuable mineral resources. General geochemical exploration methods are restricted in this region due to the thick loess overburden. Here, we used geogas prospecting, which has been uniquely developed in China, to test its ability to delineate buried deposits at Shenjiayao gold deposit. Two different media: 5% ultrapure aqua regia and polyurethane foam, were used to sample the geogas in the soil. Based on concentrations and precision in our experiment, the polyfoam seemed to out-perform the aqua regia. To investigate how the anomalies formed, a special carrier was used to sample original substances in the geogas. Nanoscale gold-bearing particles were found both in the geogas, supporting the hypothesis that metallic nanoparticles released from orebodies and altered rocks during weathering process can be transported towards the surface. Besides the evidence of nanoparticles, correlations of elements in ores and geogas indicated the close connection between them. Therefore, our field experiment showed geogas prospecting can be effective in exploration for buried mineral resources.

1. Introduction

Traditional techniques of geochemical exploration sometimes can't work effectively when target areas potentially hosting economic mineral resources are buried by transported overburden such as alluvium or loess (Cheng, 2012). Sampling of regolith materials in search of anomalous metal concentration is a key technique for locating concealed ore bodies (Anand et al., 2007). With the development of sampling and analytical techniques, researchers conjectured that ultrafine metals or metalloids in form of atoms, ions and nanoparticles deriving from orebodies could entrain the micro-flow of the geogas (ascending gas from mantle degassing, bacterial and oxidation processes, defined by (Malmqvist and Kristiansson, 1984)), and go upwards through fractures or poral spaces of rocks. Finally, they were partly trapped in soil geochemical barriers (absorbed by clays, Fe/Mn oxides, etc.) and partly remained in pores of soils (Wang et al., 2016a; Wang et al., 2016b). This hypothesis was not evaluated fully until Wang and Ye (2011) found Cu-bearing nanoparticles from the geogas and soil samples in concealed deposit. Since then, nanoparticles have attracted lots of attention and been supposed to be stable in nature based on their similarity in morphology and structure (Lu et al., 2017). Wang et al. (2017) and Ye et al. (2015) observed Au-bearing nanoparticles at gold and Ag-polymetallic deposits, respectively, and they also found Ni-Cr

bearing nanoparticles at a Cu-Ni deposit buried 140–400 m below the surface (Wang et al., 2012). Lu et al. (2017) concluded that nanoparticles in the geogas have a good correspondence with ore components and many other studies have proven this as well (Dai et al., 2015; Hu et al., 2015a; Hu et al., 2015b; Luo et al., 2015; Wei et al., 2013; Zhang et al., 2015). It was supposed that mineralization types can be deduced through compositions of geogas nanoparticles (Cao et al., 2009; Wei et al., 2013).

Geogas prospecting was evolved from the “deep-penetrating geochemistry project” launched in 1999 undertaken by several international institutes and companies. Geochemists, represented by Xuejin Xie of IGGE made great progress in extraction and analysis methods in which ultralow concentrations of trace elements could be determined. Additionally, Geochemical Mapping and China Geochemical Baseline Project promoted the development of geochemical exploration in China. Therefore, a series of deep-penetrating geochemical exploration methods develop well in China. Geogas prospecting is one of them but its sampling media and technique are very special. We sampled the geogas existing in poral spaces of soil, which was thought to contain materials from buried ores. We say geogas sampling, but actually we want to sample what exists in the geogas, therefore it is apparently different from gas exploration. Geogas prospecting was proven to be a viable tool to identify deeply buried copper deposit under alluvium and

* Corresponding author.

E-mail address: yerong@cugb.edu.cn (R. Ye).

<https://doi.org/10.1016/j.gexplo.2018.11.015>

Received 14 March 2018; Received in revised form 7 November 2018; Accepted 26 November 2018

Available online 28 November 2018

0375-6742/ © 2018 Elsevier B.V. All rights reserved.

diluvium (Wan et al., 2017).

Previous studies rarely involve gold deposit under thick loess layer except authors' study (Wang et al., 2016a). The loess land in China covers 632,000 km², occupying approximately 6% of the total, thus there is potential for discovering buried mineral resources in those areas (Yu et al., 1998). In this paper, we targeted geogas prospecting in loess-covered area using active pump method. In particular, we evaluated the relative effectiveness of using two different media to sample geogas, utilized geospatial plotting of the data to elucidate geochemical anomalies, and also studied the nanoparticles using the transmission electron microscope (TEM) with Energy Dispersive Spectroscopy (EDS). In the end all the data were analyzed in statistical method to evaluate the overall efficacy of the geochemical exploration technique used here.

2. Study area

The Shenjiayao gold deposit (gold reserve 3.8 t of grading 5.1 g/t) is located in the Xiaqingling–Xiong'ershan region which ranks the second place in gold resource of > 400 t and the third in gold production of 16.5 t annually in China (Mao et al., 2002). Gold minerals occur in quartz veins and highly altered fracture zones. Principal ore minerals include: native gold, electrum, pyrite, chalcopyrite, galena, sphalerite, arsenopyrite, marmatite. Gangue minerals include: quartz, sericite, siderite, dolomite, calcite, chlorite, barite and kaolinite. Gneiss, plagiogranitic gneiss, granodioritic rocks of the Taihua group hosts the deposit. The largest Au-bearing vein is about 5430 m long and 1–19 m thick with 265° striking and dipping to the south at 31°. NNW-trending faults/fractures control the mineralization and the intersections of NNW- and NS-faults/altered fracture zones host most of the ores. Whether it belongs to orogenic gold deposit is highly disputed (Chen and Fu, 1992; Mao et al., 2002). The deposit is covered by a 22.9–72.9 m thick loess.

3. Sampling and analyses

3.1. Sampling

We prepared 10% aqua regia solution by mixing concentrated hydrochloric acid and nitric acid (purity ≥ 99.8%) in a molar ratio of 3:1 with pure water (resistivity: 18 MΩ·cm) at the Geochemistry Lab of China University of Geoscience (Beijing). Two hundred polyurethane foam cylinders were washed two times by pure water and then soaked in the 10% aqua regia for 12 h to reduce element contents therein. Subsequently we washed these foam cylinders three times by deionized water and dried them. Finally, all foam cylinders were transferred to the 5% ultrapure aqua regia. Purpose of processing polyfoam cylinder was to improve its chemical absorption ability in addition to its natural physical absorption. Capture devices, plastic tweezers, bottles and zip lock bags were processed like the polyurethane foam cylinders in the geochemical lab. The 5% ultrapure aqua regia used for sampling and soaking foams was prepared in the Isotope Laboratory of the Institute of Geology for Nuclear Industry in Beijing for guaranteeing its purity.

Four parallel sampling lines, spaced 100 m apart, were arranged roughly perpendicular to the strike of the known gold orebodies in the Shenjiayao deposit. 41 sites were sampled in each line, with a sampling spacing of 40 m (Fig. 1). On basis of experiences of geochemical exploration, there is usually no contamination 20 cm below the soil surface. Firstly, a vertical hole was drilled into the ground to a depth of about 80 cm (60 cm if it was hard to drill) using a steel bar, and then the auger drill was instantly screwed into the hole to stop the air from escaping (Fig. 2). Subsequently, the 0.45-μm millipore filter, capture device and air pump were connected by several rubber tubes in order. Finally, A total of 3 L geogas was pumped from each hole at a slow and uniform rate. When geogas passed the foam, what carried by geogas would be captured in the foam. Each foam cylinder was conserved in the capture device and then carefully moved to a small plastic bag using

plastic tweezers. On each site two meters away from the foam sampling site the upper steps were repeated but the foam was replaced with a U-tube filled with 20 ml ultrapure 5% aqua regia. The liquid samples were transferred to plastic bottles carefully. We irrigated the U-tube using ultrapure 5% aqua regia before sampling on the next site. On some chosen sampling sites where the orebodies lay below, a larger plastic pipe with Ge-grids was set to collect geogas-carried materials for the following observation under transmission electron microscope.

A total of 168 foam samples and 168 aqua regia samples (163 normal samples, 3 repeated samples and 2 blanked samples) was collected. In addition, there was underground mining in northeast of our study area, where we collected several ore samples.

3.2. Analyses

3.2.1. Chemical analysis

Based on the previous experience of deep-penetrating geochemical exploration and geological condition in our study area, we chose 12 kinds of elements to detect their concentration: Au, Ag, As, Bi, Cu, Hg, Mo, Pb, Sb, Sn, W, and Zn. Our ore, foam and liquid samples were analyzed in the Institute of Geophysical and Geochemical Exploration (IGGE). Different methods were applied to detect different elements described in Table 1. The foam samples were put in specific tubes with 5 ml HNO₃ and 1 ml H₂O₂ and digested in microwave digestion system for 1 h. After cooling down to room temperature, they were moved to colorimetric tubes and diluted with ultrapure water to 10.0 ml to determine their concentrations. The foam, as one sort of capture media used in geogas prospecting, is so special that there is no standard material to evaluate the analysis accuracy. However, five laboratory replications were inserted into each batch of 50 samples in addition to three field replications for precision control. Results of foam samples were converted to absolute mass (ng or μg), while the unit of aqua regia samples was ng/ml. Ore samples were crushed and mashed until smaller than 0.074 mm. Detailed processes of analysis are not open for public. IGGE excels at the analysis of geochemical samples and all the determinations of our samples passed the repeatability test.

3.2.2. TEM analysis

Ge-grids placed in the plastic pipe could be directly observed under the TEM. The TEM is equipped with EDS (Energy dispersive spectroscopy) to determine elemental category. Detailed observation and determination ability of TEM was described in Lu et al., 2017.

4. Results

Element concentrations were divided into seven groups and expressed in the way of contoured maps (Figs. 3 and 4) based on their cumulative frequency: < 15% (in dark blue), 15–50% (blue), 50–75% (light blue), 75–85% (light green), 85–92% (light yellow), 92–98% (orange) and > 95% (red).

4.1. Foam samples

The relative deviations (RD%) of duplicated samples were listed in Table 2 and calculated through the following equation:

$$RD\% = |C1 - C2| / [(C1 + C2) / 2] * 100\%$$

where C1 and C2 represented the first and second determination value, respectively.

The results of analysis would be considered acceptable when the RD % is ≤ 50% according to the standard of geochemical survey projects in China. Most elements met the lowest request of RD% except As. Average or median values of Ag, Hg and Sn were smaller than corresponding blank values probably due to their ultralow concentrations, and at the same time, we need to do more work to improve the ability of chemical determination. In general, 85% of cumulative frequency can

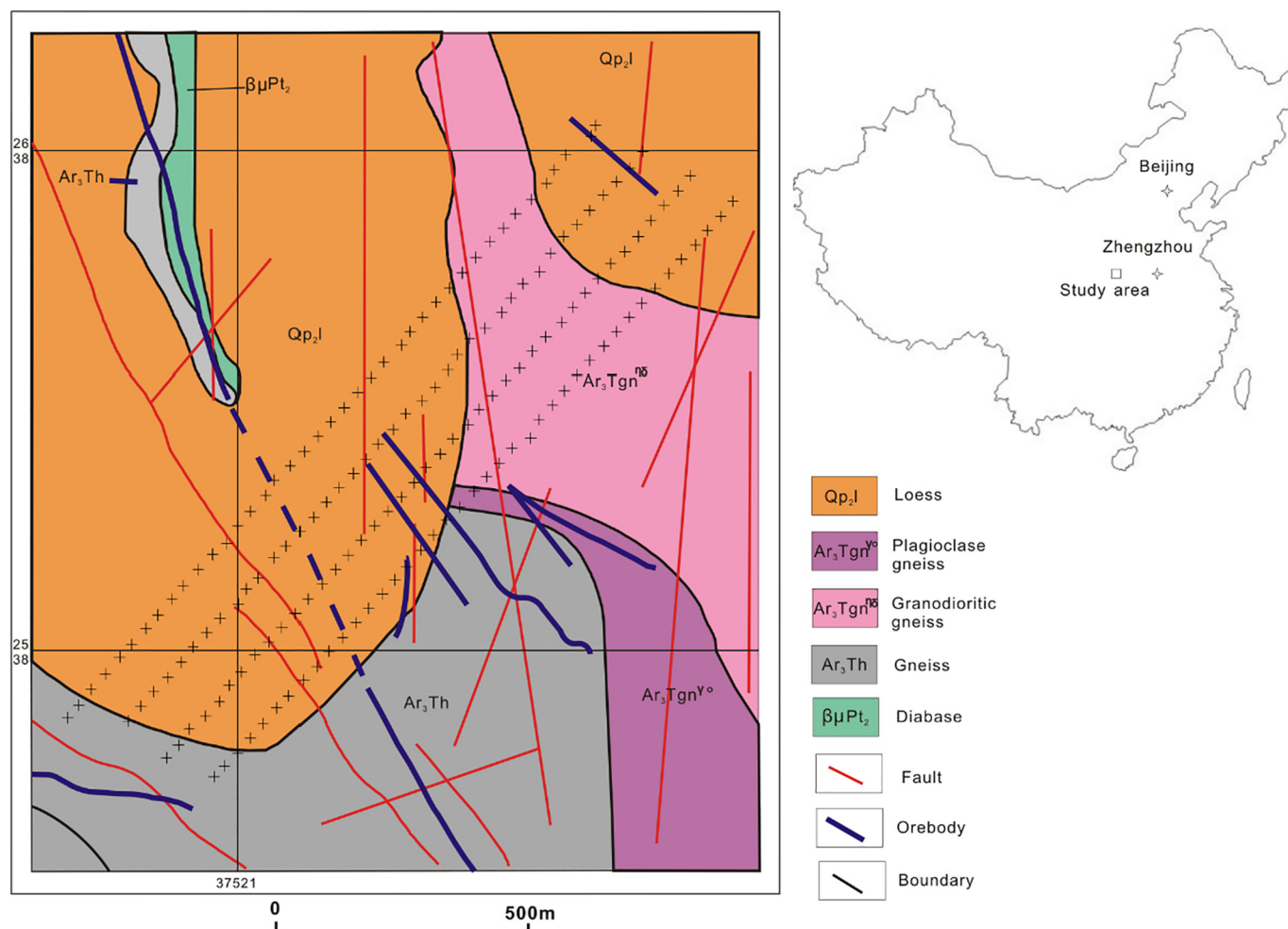


Fig. 1. Simplified geological-tectonic map and sampling points (+ marks) in the Shenjiayao gold deposit (modified after Gao, 2009).

be regarded as the lower limit of geochemical anomaly according to general experiences. However, the establishment of geochemical anomaly is very complicated and usually impacted by many factors. Geogas prospecting has not built the standard of geochemical anomalous threshold due to its special sampling media and ultralow contents. Therefore, we listed several sets of cumulative frequencies to contour spatial distributions of foam samples. Most elements in polyfoam showed greatest concentrations on the SW of the study area except Hg and Sn (Appendix Fig. 1). For example, Au formed three NNW-direction zones of high concentrations from SW to NE on the contoured map. These high-value areas were parallel ore bodies and NNW-striking faults.

4.2. 5% aqua regia samples

Table 3 showed that all results met the lowest request of RD%. However, averaged contents of As, Hg, Mo, Sn and W were close or even smaller than their blank values because of their low concentrations in the geogas or the nature of each element itself.

12 kinds of elements collected in 5% ultrapure aqua regia could exhibit several zones of high concentrations in the contoured maps as well (e.g. Au, other elements are in Appendix Fig. 2) but these high values formed several single zones rather than constituted linear areas with NNW direction. However, some high-content areas were still located above the orebodies.

We should note that only two blank samples were inserted during field sampling, and sometimes one of them had much greater concentration than our samples. However, two blank samples were rarely

high together, especially for aqua regia samples. Foams might not be totally homogenized so that there were some high-concentration samples in our experiment. Although there were some issues in results due to the low concentrations, combination of all the elements can be applied to explain results. At the same time, more precise analysis is needed for ultralow-concentration samples and more blank samples are needed to evaluate analytical quality.

4.3. Metallic nanoparticles

We detected nanoparticles in the geogas. Some of them occurred as single grains, and some small nanoparticles formed aggregations. A single nanoparticle was several to hundreds of nanometers in diameter. Spherical, granular, oval, and polygonal shapes were very common. We also observed ordered internal structure of nanoparticles indicating that they experienced crystallization. Nanoparticles had varied compositions (Table 4), like: 1) Cu; 2) Au with associated Cu; 3) Cu with other elements like Ag, Fe, Pb, Zn, Mg, Ti, V, Mo and S. The photographs below showed complex nanoparticles like Cu-Au (Fig. 5) and Cu-Au-Ag-Mg-Fe-S nanoparticles (Fig. 6).

4.4. Correlation analysis

Five ore samples showed 12.45 g/t Au and 330.42 g/t Ag averagely. Correlation analysis of compositions of ores showed that Au and W, Pb and Sb had significant correlations, respectively. These elements in foam samples exhibited significant correlations as well. It is notable that they have significant correlations in ores but also in geogas.

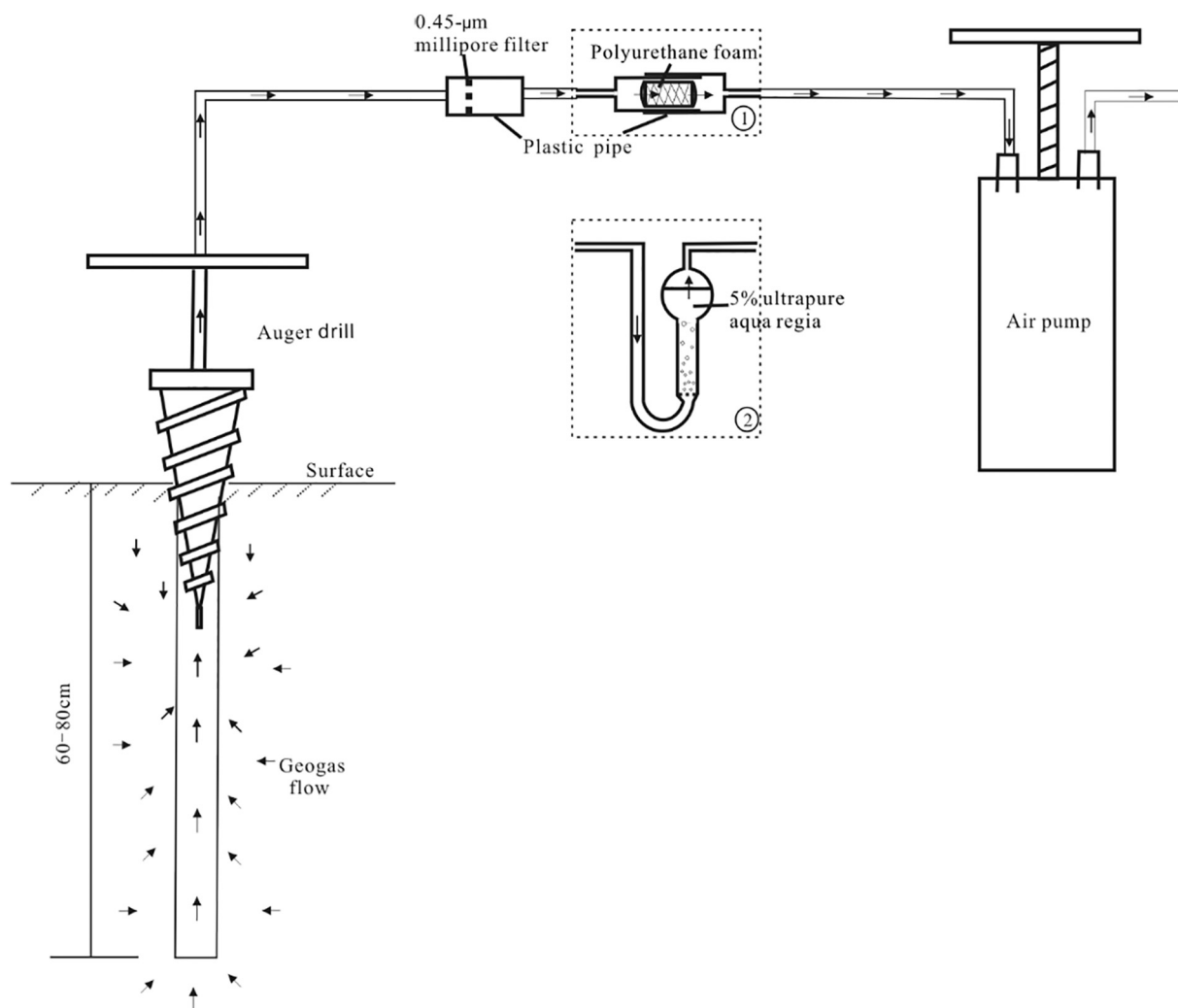


Fig. 2. The equipment and steps of geogas sampling. Black arrows represent the geogas which moves from the hole and its nearby areas through the sampling devices until it was pumped to the air. Polyurethane foam was placed in a plastic pipe like ① and ultrapure 5% aqua regia was set in a U-tube like ②.

Table 1
Analytical methods and detection limits of selected elements in the geogas and ores.

Element	Analytical method	Detection limit	Unit	Analytical method	Detection limit	Unit
Aqua regia samples			Ores samples			
Au	HR-ICP-MS	0.005	ng/ml	AAN	0.2	ng/g
				AAS	100	ng/g
Ag	HR-ICP-MS	0.01	ng/ml	ES	20	ng/g
As	HG-AFS	0.4	ng/ml	HG-AFS	0.2	µg/g
Bi	HR-ICP-MS	0.002	ng/ml	ICP-MS	0.05	µg/g
Cu	HR-ICP-MS	0.059	ng/ml	ICP-MS	1	µg/g
Hg	CV-AFS	0.003	ng/ml	CV-AFS	2	ng/g
Mo	HR-ICP-MS	0.007	ng/ml	ICP-MS	0.2	µg/g
Pb	HR-ICP-MS	0.069	ng/ml	ICP-MS	2	µg/g
Sb	HR-ICP-MS	0.01	ng/ml	ICP-MS	0.05	µg/g
Sn	HR-ICP-MS	0.128	ng/ml	ES	1	µg/g
W	HR-ICP-MS	0.008	ng/ml	ICP-MS	0.2	µg/g
Zn	HR-ICP-MS	0.317	ng/ml	ICP-MS	2	µg/g

Analytical methods: HR-ICP-MS: high resolution inductively coupled plasma mass spectrometry; HG-AFS: hydride generation atomic fluorescence spectrum; CV-AFS: cold vapor atomic fluorescence spectrum; AAN: flameless atomic absorption spectroscopy; AAS: atomic absorption spectroscopy ES: emission spectroscopy; ICP-MS: inductively coupled plasma mass spectrometry.

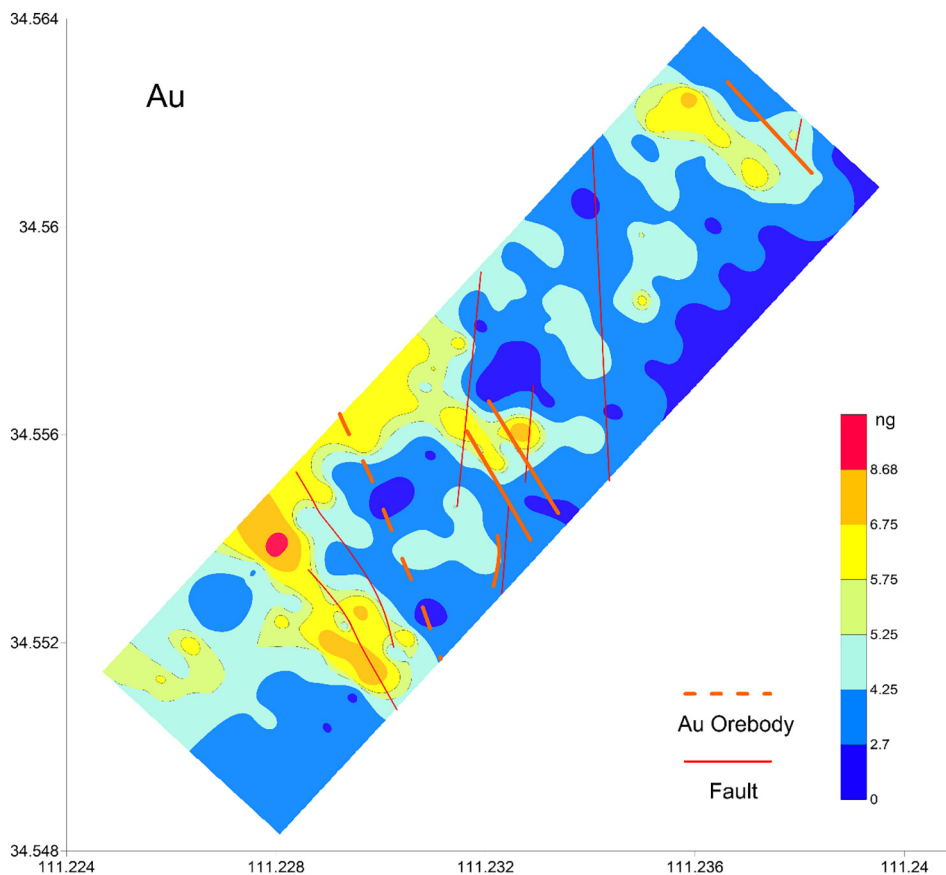


Fig. 3. Geochemical maps of Au in the polyurethane foam.

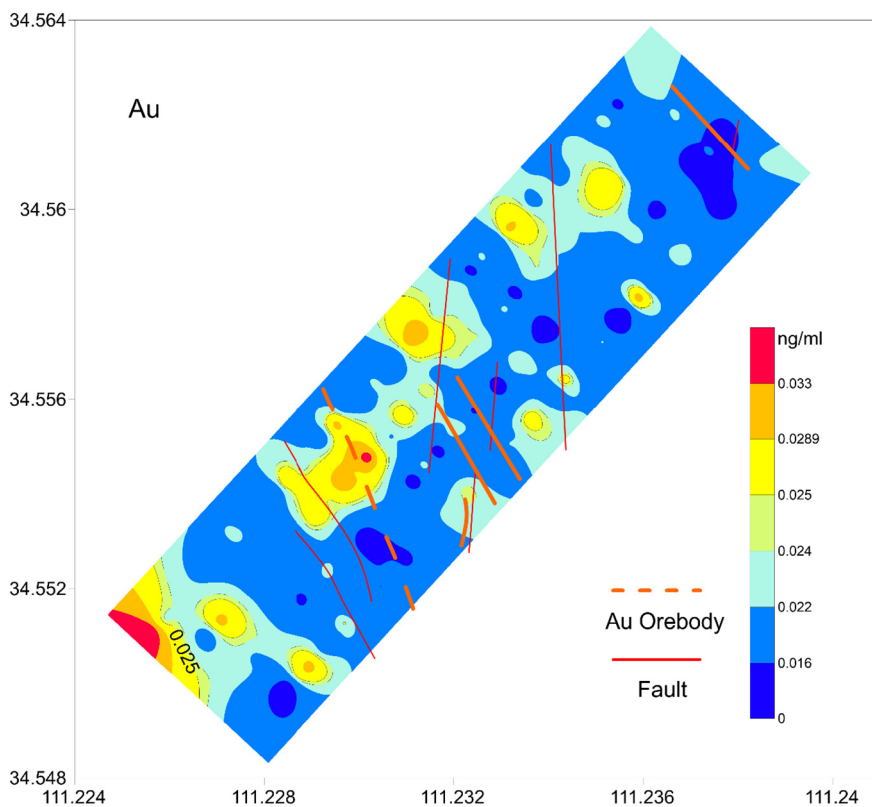


Fig. 4. Geochemical maps of Au in the 5% ultrapure aqua regia.

Table 2Average, median, 85% cumulative frequency, relative deviation values of polyurethane foam samples. Unit is μg except what's labeled.

Parameters	Au(ng)	Ag(ng)	As	Bi	Cu	Hg(ng)	Mo	Pb	Sb	Sn(ng)	W	Zn
Average	4.32	5.86	1.26	0.0052	1.22	6.70	0.015	0.36	0.011	7.42	0.014	1.25
Median	4.25	5.50	0.05	0.0030	0.13	5.13	0.014	0.32	0.008	7.36	0.011	0.89
85% frequency	5.75	7.75	6.05	0.0094	0.42	9.85	0.021	0.44	0.015	8.66	0.022	2.12
RD%	34.09	26.47	74.62	28.90	39.07	45.78	29.35	11.21	30.57	5.26	30.08	29.92
Blank1	3.00	6.00	0.10	0.0029	0.09	8.25	0.014	0.32	0.004	9.02	0.010	0.57
Blank2	4.00	16.75	0.01	0.0017	0.06	0.63	0.016	0.23	0.005	0.30	0.007	0.64

Table 3

Average, median, 85% cumulative frequency, relative deviation values of samples in 5% ultrapure aqua regia. Unit: ng/ml.

Parameters	Au	Ag	As	Bi	Cu	Hg	Mo	Pb	Sb	Sn	W	Zn
Average	0.022	0.06	0.288	0.022	1.669	0.034	0.051	1.15	0.32	0.693	0.040	19.98
Median	0.021	0.06	0.398	0.030	4.939	0.039	0.058	2.65	0.57	0.856	0.049	31.02
85% frequency	0.025	0.09	0.634	0.041	3.838	0.051	0.079	1.71	1.10	0.878	0.065	36.26
RD%	31.07	31.05	25.00	15.70	16.90	24.58	32.49	9.29	17.80	19.87	21.44	14.51
Blank1	0.02	0.03	0.29	0.013	1.43	0.028	0.054	0.86	0.09	0.600	0.020	3.20
Blank2	0.02	0.02	0.29	0.012	1.00	0.033	0.060	0.85	0.08	0.762	0.193	3.47

Table 4

Characteristics of nanoparticles in geogas of Shenjiayao gold deposit.

Shape	Sphere, oval, polygon
Diameter	Several to hundreds of nm
Structure	Ordered internal structure
Composition	Cu-Au, Cu-Pb-Au, Cu, Cu-Ti-Fe-Mo, Cu-Fe, Cu-Fe-Zn-Ti-V, Mn-Fe, Cu-Ti, Fe-Zn, Cu-Au-Ag-Mg-Fe-S
Assemblage form	Single pellets, chain, irregular pellets, aggregation

Additionally, Ag and Pb are significantly correlated in ores and 5% aqua regia samples.

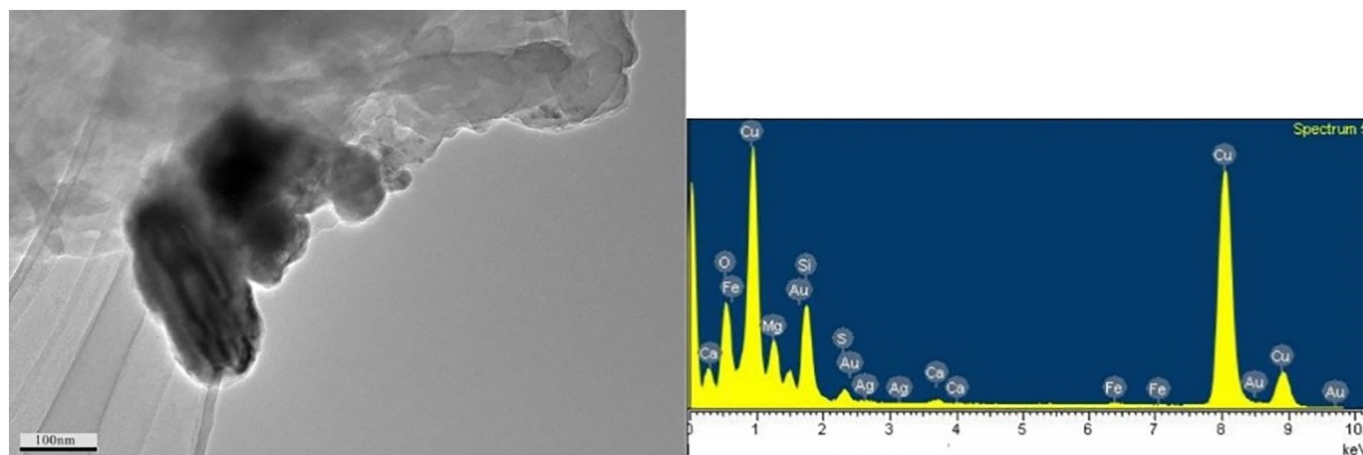
5. Discussion

Polyurethane foam and 5% ultrapure aqua regia were utilized to capture materials in the geogas. For foam samples, we used microwave digestion rather than regular ashing method to minimize the loss of some elements which could not keep stable in high temperature (Yan et al., 2016). Hg and Sn concentrations might be extremely low in the geogas so that their average values were smaller than blank values. Foam samples had much higher concentrations than aqua regia samples when concentrations were transferred to absolute mass, indicating foams had stronger ability to capture what in geogas than 5% aqua regia. High-value areas of the foam samples were more obvious than

those of the 5% aqua regia, and furthermore these areas formed several linear contoured areas paralleling orebodies and NNW-trending faults. Based on their spatial distribution it can be deduced that high concentrations of geogas were induced by deep mineralization and faults. The deep mineralization can provide the ore-related elements and the faults can provide beneficial spaces for geogas transporting. Therefore, we suggest that processed polyurethane foam is the better medium for geogas prospecting.

High concentration areas surrounded by low concentrations usually occurred on the SW of geospatial maps which is the location of the largest concealed ore body at Shenjiayao gold deposit. Meanwhile on the central and northeastern part some elements also presented high concentration centers. Comparing the locations of positive anomalies and actual orebodies, it was not hard to find out that anomalous area were usually located on the left of the direction where orebodies were projected to the horizontal. Considering that the largest Au-bearing belt was NNW-striking and dipped to the SW over 1 km long along the dip direction, it could be explicated that when geogas passed through the ore bodies, carried ore-related materials, and unloaded these materials on the surface, high concentration areas would occur on the projection positions of orebodies (Figs. 3 and 4).

That several elements showed significant correlation in ores and geogas indicated elements in geogas samples may inherit the characteristics of those in ores. Shenjiayao gold deposit should enrich in Au, Cu, Pb, Zn and Ag in terms of its primary ore minerals, meanwhile these

**Fig. 5.** Cu-Au-Ag-Mg-Fe-S bearing nanoparticles in geogas in Shenjiayao gold deposit.

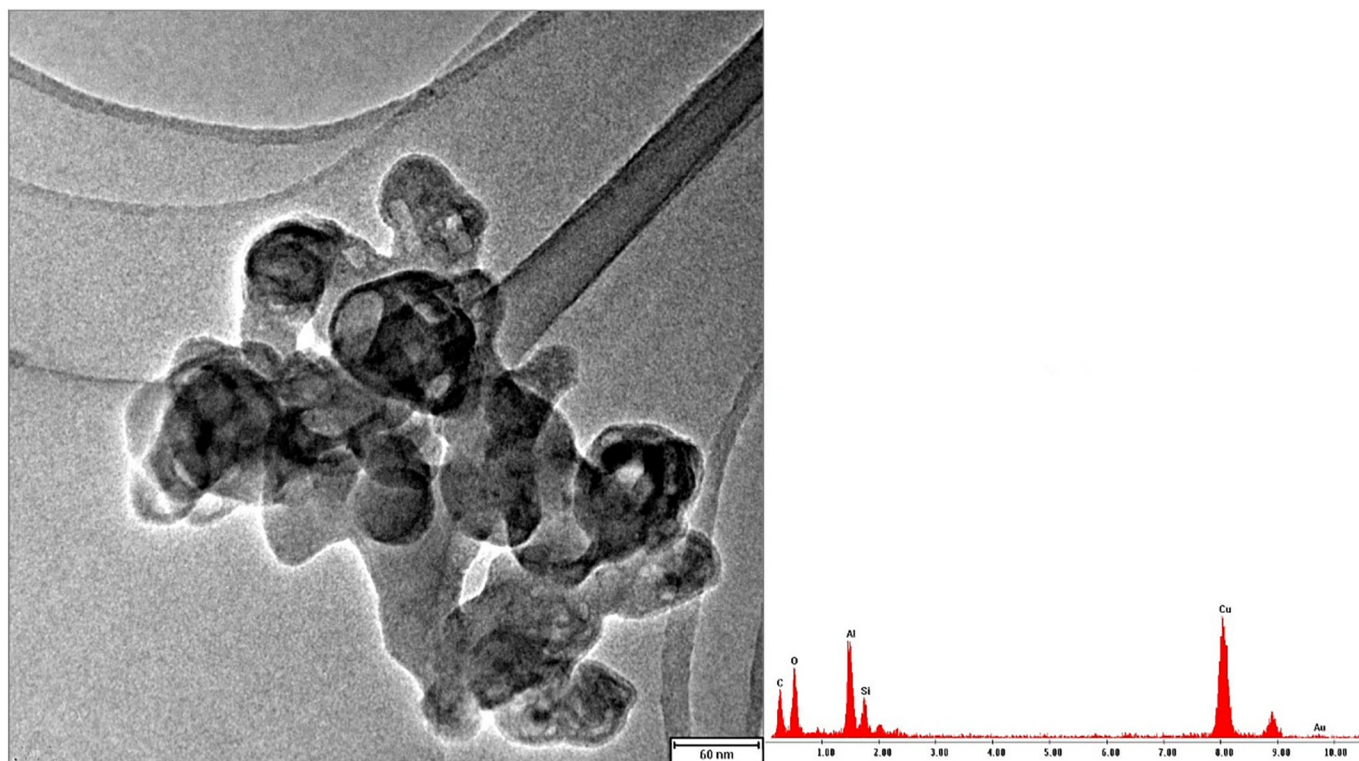


Fig. 6. Cu-Au bearing nanoparticles in geogas in Shenjiayao gold deposit.

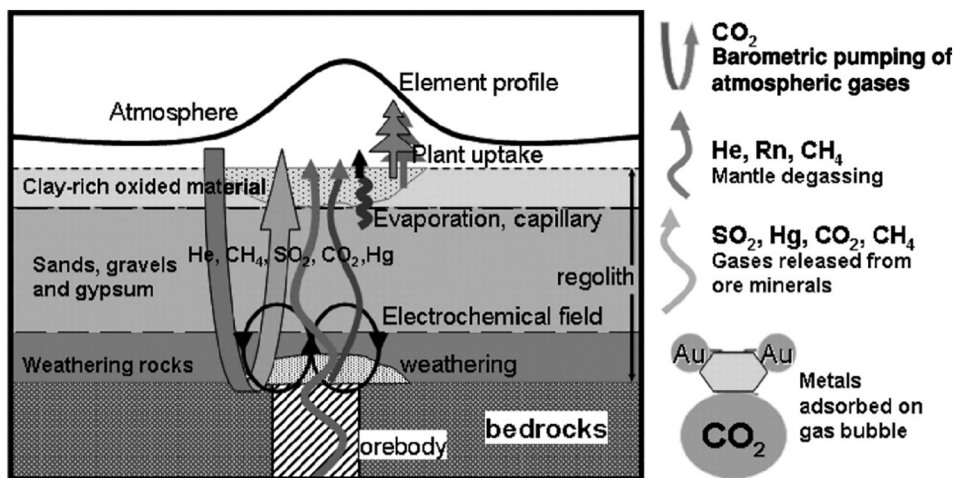


Fig. 7. Conceptual migration model of ore related elements in the desert regolith profile (Wang et al., 2007).

elements are also rich in geogas, presenting some compositional connections between ores and geogas. Au, Cu, Pb, Zn, Ag and Fe-bearing nanoparticles were also found in geogas. The similarities of chemical compositions, spatial correspondence between anomalies and actual ore bodies, and Au-bearing nanoparticles discovered in the geogas together form a close chain to support that nanoparticles, the primary substances in geogas, are originated from concealed deposit.

Unlike previous studies on geogas prospecting in which only nanoparticles were sampled and analyzed, we also utilized foam and aqua regia to capture what in the geogas and then plotted geospatial maps. Thus, when positive anomalies were identified on the geochemical maps and then applied to reveal the buried ore bodies, not only nanoparticles containing ore-related elements did verify the connection between anomalies and ore deposit, but they also explained what anomalies are and how they formed.

Wang et al., 2012 set a 2 m long simulation tube with several holes

in the bottom in the lab. Ores, sands and soils were filled in the tube from the bottom to the top. They sampled soils regularly and after 16 months, they discovered gold-bearing and Cu-bearing nanoparticles in soils. It well supported that heavy elements can be transported with the ascending gas. Wang et al. (2007) described the migration model of geogas in desert terrains (Fig. 7). It was thought that nanoscale gold particles may migrate vertically with the gas flow and could be observed in the geogas and soil (Wang et al., 2016b, 2017, Zhang et al., 2016). We also observed Au-bearing nanoparticles in geogas, which strongly supported this hypothesis. Saunders et al. (2016) proposed that Au, Ag and Cu can form nanoparticles in the deep earth and then move physically to epithermal environment. Whether nanoparticles formed in ore-forming process could benefit the discovery of nanoparticles in geogas needs further research.

6. Conclusions

These are the conclusions we would elaborate on:

- 1) Both the polyurethane foam and 5% aqua regia media of sampling the geogas showed promising results for delineating the occurrence of ore bodies buried under loess. However, the foam seemed to work better than the aqua regia, but both showed some promise for deep prospecting in loess-covered areas.
- 2) Results presented here show that metallic nanoparticles are released from deep ore bodies. Thus, the documentation of the nanoparticles of the elements of economic interest that were entrained in soil gas suggests they might be used for geochemical exploration as well, but more research is required to evaluate that.
- 3) Significant geochemical correlations between Au and W, Pb and Sb, and Ag and Pb in ores and geogas indicate that the geogas derived from ores inherits at least some of their characteristics.

Use of geogas exploration techniques have been shown here to be effective in discriminating the location of ore mineralization buried under a relatively thick cover of loess. More research on the exact mechanism of nanoparticles release from mineral deposit appears warranted, as does evaluation of how to use the technology for regional-scale exploration.

Acknowledgments

We thank Dr. Saunders of Auburn University for his constructive advice. We also appreciate Hannah Smith of Miller Writing Center and Dr. Saunders in Auburn University for the help in language. Dr. Martiya is thanked for the review and helpful suggestions. This study is supported by the Natural Science Foundation of China (grant numbers 41573037, 41273063), National Key Research and Development Project (grant number 2016YFC0600602-2) and Fundamental Research Funds for the Central Universities (grant number 2652016075). Mei Lu also wants to thank China Scholarship Council for supporting her study in Auburn University.

Appendix A. Supplementary data

Supplementary data to this article can be found online at <https://doi.org/10.1016/j.gexplo.2018.11.015>.

References

- Anand, R.R., Cornelius, M., Phang, C., 2007. Use of vegetation and soil in mineral exploration in areas of transported overburden, Yilgarn Craton, Western Australia: a contribution towards understanding metal transportation processes. *Geochem. Explor. Environ. Anal.* 7, 267–288.
- Cao, J.J., Hu, R.Z., Liang, Z.R., Peng, Z.L., 2009. TEM observation of geogas-carried particles from the Changkeng concealed gold deposit, Guangdong Province, South China. *J. Geochem. Explor.* 101 (3), 247–253.
- Chen, Y.J., Fu, S.G., 1992. Mineralization model and geological-geochemical features of the Shenjiayao gold deposit. *Geophys. Prospect.* 04, 47–52 (in Chinese with English abstract).
- Cheng, Q.M., 2012. Ideas and methods for mineral resources integrated prediction in covered areas. *Earth Sci. J. China Univ. Geosci.* 37 (6), 1109–1125 (in Chinese with English abstract).
- Dai, D.L., Cao, J.J., Lai, P.X., Wu, Z.Q., 2015. TEM study on particles transported by ascending gas flow in the Xakiutata iron deposit, Inner Mongolia, North China. *Geochem. Explor. Environ. Anal.* 15, 255–271.
- Gao, Y., 2009. Practice on Synthetic Exploration Methods and Techniques on Hidden Endogenesis Metal Deposits in west Henan Province. China University of Geosciences (Beijing) for doctoral degree. (in Chinese with English abstract).
- Hu, G., Cao, J.J., Lai, P.X., Hopke, P.K., Holub, R.F., Zeng, J.N., Wang, Z.H., Wu, Z.Q., 2015a. Characteristics and geological significance of particles on fractures from the Dongshengmiao polymetallic pyrite deposit, Inner Mongolia, China. *Geochem. Explor. Environ. Anal.* 15, 373–381.
- Hu, G.A., Cao, J.J., Hopke, P.K., Holub, R.F., 2015b. Study of carbon-bearing particles in ascending geogas flows in the Dongshengmiao polymetallic pyrite deposit, Inner Mongolia, China. *Resour. Geol.* 65, 13–26.
- Lu, M., Ye, R., Zhang, B.M., Yao, W.S., Han, Z.X., 2017. Occurrence and formation of metallic nanoparticles over the concealed ore deposits. *J. Nanosci. Nanotechnol.* 17 (9), 6077–6082.
- Luo, S.Y., Cao, J.J., Yan, H.B., Yi, J., 2015. TEM observations of particles based on sampling in gas and soil at the Dongshengmiao polymetallic pyrite deposit, Inner Mongolia, Northern China. *J. Geochem. Explor.* 158, 95–111.
- Malmqvist, L., Kristiansson, K., 1984. Experimental-evidence for an ascending microflow of geogas in the ground. *Earth Planet. Sci. Lett.* 70, 407–416.
- Mao, J.W., Goldfarb, R.J., Zhang, Z.W., Xu, W.Y., Qiu, Y.M., Deng, J., 2002. Gold deposits in the Xiaqingling-Xiong'ershan region, Qinling Mountains, central China. *Mineral. Deposita* 37 (3–4), 306–325.
- Saunders, J.A., Mathur, R., Kamenov, G.D., Shimizu, T., Brueske, M.E., 2016. New isotopic evidence bearing on bonanza (Au-Ag) epithermal ore-forming processes. *Mineral. Deposita* 51 (1), 1–11.
- Wan, W., Wang, M.Q., Hu, M.Y., Gao, Y.Y., 2017. Identification of metal sources in geogas from the Wangjiazhuang copper deposit, Shandong, China: evidence from lead isotopes. *J. Geochem. Explor.* 172, 167–173.
- Wang, X.Q., Ye, R., 2011. Finding of nanoscale metal particles: evidence for deep-penetrating geochemistry. *Acta Geol. Sin.* 32, 7–12 (in Chinese with English abstract).
- Wang, X.Q., Wen, X., Ye, R., 2007. Vertical variations and dispersion of elements in arid desert regolith: a case study from the Jinwozi gold deposit, northwestern China. *Geochem. Explor. Environ. Anal.* 7, 163–171.
- Wang, X.Q., Zhang, B.M., Liu, X.M., 2012. Nanogeochemistry: Deep-penetrating geochemical exploration through cove. *Earth Sci. Front.* 19 (3), 101–112 (In Chinese with English abstract).
- Wang, X.J., Lu, M., Wang, Z.K., Ye, R., 2016a. Characteristics of geogas anomalies measured in the Shenjiayao gold deposit of Shan County, Henan Province. *Geol. Explor.* 52 (4), 667–677 (in Chinese with English abstract).
- Wang, X.Q., Zhang, B.M., Lin, X., Xu, S.F., Yao, W.S., Ye, R., 2016b. Geochemical challenges of diverse regolith-covered terrains for mineral exploration in China. *Ore Geol. Rev.* 73, 417–431.
- Wang, X.Q., Zhang, B.M., Ye, R., 2017. Nanoparticles observed by TEM from gold, copper-nickel and silver deposits and implications for mineral exploration in covered terrains. *J. Nanosci. Nanotechnol.* 17 (9), 6014–6025.
- Wei, X.J., Cao, J.J., Holub, R.F., Hopke, P.K., Zhao, S.J., 2013. TEM study of geogas-transported nanoparticles from the Fankou lead-zinc deposit, Guangdong Province, South China. *J. Geochem. Explor.* 128, 124–135.
- Yan, H.Z., Sun, B.B., Xu, J.L., Zhou, G.H., He, L., Liu, Y.F., Wang, T.Y., 2016. Comparisons of ashing and microwave digestion in analyzing geochemical polyurethane foam samples. In: *Rock and Mineral Analysis.* 35(3). pp. 276–283 (in Chinese with English abstract).
- Ye, R., Zhang, B.M., Wang, Y., 2015. Mechanism of the migration of gold in desert regolith cover over a concealed gold deposit. *Geochem. Explor. Environ. Anal.* 15 (1), 62–71.
- Yu, X.D., Li, Y.G., Yang, S.P., Cheng, H.X., Zhao, C.D., 1998. The tracing studies of buried gold deposits in thick loess overburden area. *Bull. Mineral. Petrol. Geochem.* 17 (3), 160–163 (in Chinese with English abstract).
- Zhang, B.M., Wang, X.Q., Ye, R., Zhou, J., Liu, H.L., Liu, D.S., Han, Z.X., Lin, X., Wang, Z.K., 2015. Geochemical exploration for concealed deposits at the periphery of the Zijinshan copper-gold mine, southeastern China. *J. Geochem. Explor.* 157, 184–193.
- Zhang, B.M., Wang, X.Q., Chi, Q.H., Yao, W.S., Liu, H.L., Lin, X., 2016. Three-dimensional geochemical patterns of regolith over a concealed gold deposit revealed by overburden drilling in desert terrains of northwestern China. *J. Geochem. Explor.* 164, 122–135.